J|A|C|S ARTICLES

Published on Web 10/01/2009

Speeding Up ^{13}C Direct Detection Biomolecular NMR Spectroscopy

Wolfgang Bermel,[†] Ivano Bertini,*[,‡] Isabella C. Felli,[‡] and Roberta Pierattelli[‡]

Bruker BioSpin GmbH, Silberstreifen, 76287 Rheinstetten, Germany, and CERM and Department of Chemistry, University of Florence, Via Luigi Sacconi 6, 50019 Sesto Fiorentino (Florence), Italy

Received July 14, 2009; E-mail: ivanobertini@cerm.unifi.it

Abstract: After the exploitation of ^{1}H polarization as a starting source for ^{13}C direct detection experiments, pulse sequences are designed which exploit the accelerated ^{1}H longitudinal relaxation to expedite ^{13}C direct detection experiments. We show here that 2D experiments based on ^{13}C direct detection on a 0.5 mM water sample of ubiquitin can be recorded in a few minutes and 3D experiments in a few hours. We also show that fast methods like nonuniform sampling can be easily implemented. As overall experimental time has always been a counter indication for the use of ^{13}C direct detection experiments, this research opens new avenues for the application of ^{13}C NMR to biological molecules.

Introduction

The intrinsically low sensitivity of NMR spectroscopy as compared to other spectroscopic techniques has always been the price to pay to have access to exquisitely detailed information on the structural and dynamic properties of molecules in solution, without perturbing their chemical properties. Multidimensional NMR experiments thus result from repetition of the basic pulse sequence for a very large number of times, and, to obtain the necessary resolution in all of the indirect dimensions, a large number of data points should be acquired. This dramatically impacts on the duration of the experiments.

This drawback of NMR spectroscopy has recently been greatly alleviated by the tremendous improvements in instrumental sensitivity brought about by the advent of high static magnetic fields as well as by the development of probeheads characterized by reduced noise,[1] both aspects contributing to an enhanced signal-to-noise ratio (S/N) of the spectra. Thanks to the increased sensitivity, several elegant strategies, partly derived from the field of magnetic resonance imaging where the duration of the NMR experiment constitutes an important issue, have been recently implemented in high-resolution biomolecular ^{1}H NMR to significantly reduce the time necessary to perform an experiment.[2,3] These strategies can be subdivided into two main categories that consist of either reducing the number of acquired data points[4−21] or reducing the interscan delay,[22−31] which are the major determinants of the duration of an NMR experiment. The implementation of these features in multidimensional inverse-detection NMR experiments has greatly contributed to a drastic reduction of the NMR time necessary to obtain a specific result. A complete series of NMR

[†] Bruker BioSpin GmbH.
[‡] University of Florence.

(1) Kovacs, H.; Moskau, D.; Spraul, M. *Prog. NMR Spectrosc.* **2005**, *46*, 131–155.
(2) Felli, I. C.; Brutscher, B. *ChemPhysChem* **2009**, *10*, 1356–1368.
(3) Schanda, P. *Prog. NMR Spectrosc.* **2009**, *55*, 238–265.
(4) Chylla, R. A.; Markley, J. L. *J. Biomol. NMR* **1995**, *5*, 245–258.
(5) Brutscher, B.; Morelle, N.; Cordier, F.; Marion, D. *J. Magn. Reson., Ser. B* **1995**, *109*, 238–242.
(6) Orekhov, V. Y.; Ibraghimov, I. V.; Billeter, M. *J. Biomol. NMR* **2001**, *20*, 49–60.
(7) Kim, S.; Szyperski, T. *J. Am. Chem. Soc.* **2003**, *125*, 1385–1393.
(8) Kupce, E.; Freeman, R. *J. Am. Chem. Soc.* **2003**, *125*, 13958–13959.
(9) Orekhov, V. Y.; Ibraghimov, I.; Billeter, M. *J. Biomol. NMR* **2003**, *27*, 165–173.
(10) Kupce, E.; Nishida, T.; Freeman, R. *Prog. NMR Spectrosc.* **2003**, *42*, 95–122.
(11) Kupce, E.; Freeman, R. *J. Am. Chem. Soc.* **2004**, *126*, 6429–6440.
(12) Atreya, H. S.; Szyperski, T. *Proc. Natl. Acad. Sci. U.S.A.* **2004**, *101*, 9642–9647.
(13) Rovnyak, D.; Frueh, D. P.; Sastry, M.; Sun, Z. Y.; Stern, A. S.; Hoch, J. C.; Wagner, G. *J. Magn. Reson.* **2004**, *170*, 15–21.
(14) Hiller, S.; Fiorito, F.; Wüthrich, K.; Wider, G. *Proc. Natl. Acad. Sci. U.S.A.* **2005**, *102*, 10876–10881.
(15) Marion, D. *J. Biomol. NMR* **2005**, *32*, 141–150.
(16) Luan, T.; Jaravine, V.; Yee, A.; Arrowsmith, C.; Orekhov, V. Y. *J. Biomol. NMR* **2005**, *33*, 1–14.
(17) Kazimierczuk, K.; Kozminski, W.; Zhukov, I. *J. Magn. Reson.* **2006**, *179*, 323–328.
(18) Mobli, M.; Maciejewski, M. W.; Gryk, M. R.; Hoch, J. C. *J. Biomol. NMR* **2007**, *39*, 133–139.
(19) Lescop, E.; Schanda, P.; Rasia, R.; Brutscher, B. *J. Am. Chem. Soc.* **2007**, *129*, 2756–2757.
(20) Jaravine, V. A.; Zhuravleva, A. V.; Permi, P.; Ibraghimov, I.; Orekhov, V. Y. *J. Am. Chem. Soc.* **2008**, *130*, 3927–3936.
(21) Maciejewski, M. W.; Qui, H. Z.; Rujan, I.; Mobli, M.; Hoch, J. C. *J. Magn. Reson.* **2009**, *199*, 88–93.
(22) Ross, A.; Salzmann, M.; Senn, H. *J. Biomol. NMR* **1997**, *10*, 389–396.
(23) Pervushin, K.; Vogeli, B.; Eletsky, A. *J. Am. Chem. Soc.* **2002**, *124*, 12898–12902.
(24) Diercks, T.; Daniels, M.; Kaptein, R. *J. Biomol. NMR* **2005**, *33*, 243–259.
(25) Schanda, P.; Brutscher, B. *J. Am. Chem. Soc.* **2005**, *127*, 8014–8015.
(26) Deschamps, M.; Campbell, I. D. *J. Magn. Reson.* **2006**, *178*, 206–211.
(27) Schanda, P.; Van Melckebeke, H.; Brutscher, B. *J. Am. Chem. Soc.* **2006**, *128*, 9042–9043.
(28) Gal, M.; Schanda, P.; Brutscher, B.; Frydman, L. *J. Am. Chem. Soc.* **2007**, *129*, 1372–1377.
(29) Kupce, E.; Freeman, B. *Magn. Reson. Chem.* **2007**, *45*, 2–4.
(30) Lescop, E.; Schanda, P.; Brutscher, B. *J. Magn. Reson.* **2007**, *187*, 163–169.
(31) Müller, L. *J. Biomol. NMR* **2008**, *42*, 129–137.

10.1021/ja9058525 CCC: $40.75

experiments to perform sequence-specific assignment of a protein has been thus reduced from a few weeks to a few days.[12,13,27,30,32−35]

Another field of research that has been greatly stimulated by the recent improvements of NMR instrumental sensitivity is direct detection of carbon-13 to study biological macromolecules.[36−38] Despite that ^{13}C nuclear spins are characterized by a reduced sensitivity as compared to proton spins, and in fact ^{1}H constitutes the nucleus of choice in NMR, ^{13}C NMR provides additional tools in all cases in which ^{1}H NMR spectroscopy finds limitations. Some examples are paramagnetic or large proteins where ^{1}H may be broadened beyond detection while (at least some) ^{13}C nuclei may still be narrow enough to provide high-resolution information,[39−51] or unfolded systems where the lack of a stable 3D structure greatly reduces the proton chemical shift dispersion.[52−55] However, ^{13}C direct detection NMR experiments may be useful also in cases where the ^{1}H detection does not suffer from counter indications, such as for all of the small/medium size proteins suitable for a complete structural and dynamic characterization through NMR, as it is able to complement, and sometimes to complete, the data obtainable by proton NMR.[56−60] In the latter case, the exploitation of ^{1}H polarization as a starting point of the NMR experiments can significantly improve the sensitivity of the experiment,[61−68] even in the case of NMR experiments where no ^{1}H chemical shift labeling occurs in any of the dimensions.[54] The leap in sensitivity lately obtained in ^{13}C NMR direct detection now permits one to fully exploit the methods introduced in NMR spectroscopy to speed up the timing of the experiments.

We will show here how with the exploitation of longitudinal relaxation enhancement[23,25−27,30,31] as well as extensive spectral aliasing,[19,69−71] a ^{13}C NMR direct detected 2D experiment can be acquired in a few minutes (a CACO[56] in 1 min and a CON[37] in 5 min) and a 3D experiment in a few hours (a CBCACON[37] in 6 h or a CANCO[72] in 11 h) on a 0.5 mM sample of ubiquitin. The experimental time of a multidimentional experiment can be further reduced with the introduction of nonuniform/sparse sampling techniques, such as multidimensional decomposition (MDD).[6,9,16,20]

This demonstrates that ^{13}C NMR direct detection is a mature technique for any kind of biomolecular application.

Experimental Data

NMR Experiments. All NMR experiments were performed at 16.4 T on a Bruker Avance spectrometer operating at 700.06 MHz ^{1}H and 176.03 MHz ^{13}C frequencies, equipped with a ^{13}C cryogenically cooled probehead optimized for ^{13}C direct detection. The experiments were acquired with a 0.5 mM ^{13}C, ^{15}N labeled ubiquitin sample in HEPES buffer at pH 7.0.

The new pulse sequences, described in detail and discussed in the following section, are shown in the Supporting Information. Common parameters used for all experiments are described in detail in this paragraph, while those specific for each experiment are reported in the captions of the figures describing the pulse sequences. Unless otherwise specified, for ^{13}C band-selective $\pi/2$ and π flip angle pulses, Q5 (or time reversed Q5) and Q3 shapes[73] were used with durations of 274 and 220 μs, respectively, except for the π pulses that should be band-selective on the C^{α} region (Q3, 860 ms) and for the adiabatic π pulse to invert both C' and C^{α} (smoothed Chirp,[74] 500 μs, 25% smoothing, 80 kHz sweep,

(32) Liu, G.; Shen, Y.; Atreya, H. S.; Parish, D.; Shao, Y.; Sukumaran, D. K.; Xiao, R.; Yee, A.; Lemak, A.; Bhattacharya, A.; Acton, T. A.; Arrowsmith, C. H.; Montelione, G. T.; Szyperski, T. *Proc. Natl. Acad. Sci. U.S.A.* **2005**, *102*, 10487–10492.
(33) Schanda, P.; Forge, V.; Brutscher, B. *Proc. Natl. Acad. Sci. U.S.A.* **2007**, *104*, 11257–11262.
(34) Kupce, E.; Freeman, R. *J. Am. Chem. Soc.* **2008**, *130*, 10788–10792.
(35) Lescop, E.; Brutscher, B. *J. Biomol. NMR* **2009**, *44*, 43–57.
(36) Bermel, W.; Bertini, I.; Felli, I. C.; Piccioli, M.; Pierattelli, R. *Prog. NMR Spectrosc.* **2006**, *48*, 25–45.
(37) Bermel, W.; Bertini, I.; Felli, I. C.; Kümmerle, R.; Pierattelli, R. *J. Magn. Reson.* **2006**, *178*, 56–64.
(38) Bermel, W.; Felli, I. C.; Kümmerle, R.; Pierattelli, R. *Concepts Magn. Reson.* **2008**, *32A*, 183–200.
(39) Kostic, M.; Pochapsky, S. S.; Pochapsky, T. C. *J. Am. Chem. Soc.* **2002**, *124*, 9054–9055.
(40) Machonkin, T. E.; Westler, W. M.; Markley, J. L. *J. Am. Chem. Soc.* **2002**, *124*, 3204–3205.
(41) Bermel, W.; Bertini, I.; Felli, I. C.; Kümmerle, R.; Pierattelli, R. *J. Am. Chem. Soc.* **2003**, *125*, 16423–16429.
(42) Machonkin, T. E.; Westler, W. M.; Markley, J. L. *J. Am. Chem. Soc.* **2004**, *126*, 5413–5426.
(43) Bertini, I.; Jiménez, B.; Piccioli, M. *J. Magn. Reson.* **2005**, *174*, 125–132.
(44) Machonkin, T. E.; Westler, W. M.; Markley, J. L. *Inorg. Chem.* **2005**, *44*, 779–797.
(45) Balayssac, S.; Jiménez, B.; Piccioli, M. *J. Biomol. NMR* **2006**, *34*, 63–73.
(46) Caillet-Saguy, C.; Delepierre, M.; Lecroisey, A.; Bertini, I.; Piccioli, M.; Turano, P. *J. Am. Chem. Soc.* **2006**, *128*, 150–158.
(47) Bermel, W.; Felli, I. C.; Matzapetakis, M.; Pierattelli, R.; Theil, E. C.; Turano, P. *J. Magn. Reson.* **2007**, *188*, 301–310.
(48) Matzapetakis, M.; Turano, P.; Theil, E. C.; Bertini, I. *J. Biomol. NMR* **2007**, *38*, 237–242.
(49) Pochapsky, S. S.; Sunshine, J.; Pochapsky, T. C. *J. Am. Chem. Soc.* **2008**, *130*, 2156–2157.
(50) Takeuchi, K.; Sun, Z. N.; Wagner, G. *J. Am. Chem. Soc.* **2008**, *130*, 17210–17211.
(51) Abriata, L. A.; Ledesma, G. N.; Pierattelli, R.; Vila, A. J. *J. Am. Chem. Soc.* **2009**, *131*, 1939–1946.
(52) Bermel, W.; Bertini, I.; Felli, I. C.; Lee, Y.-M.; Luchinat, C.; Pierattelli, R. *J. Am. Chem. Soc.* **2006**, *128*, 3918–3919.
(53) Hsu, S. T.; Bertoncini, C. W.; Dobson, C. M. *J. Am. Chem. Soc.* **2009**, *131*, 7222–7223.
(54) Bermel, W.; Bertini, I.; Csizmok, V.; Felli, I. C.; Pierattelli, R.; Tompa, P. *J. Magn. Reson.* **2009**, *198*, 275–281.
(55) Knoblich, K.; Whittaker, S.; Ludwig, C.; Michiels, P.; Jiang, T.; Schafflhausen, B.; Günther, U. *Biomol. NMR Assign.* **2009**, *3*, 119–123.
(56) Bermel, W.; Bertini, I.; Duma, L.; Emsley, L.; Felli, I. C.; Pierattelli, R.; Vasos, P. R. *Angew. Chem., Int. Ed.* **2005**, *44*, 3089–3092.
(57) Babini, E.; Felli, I. C.; Lelli, M.; Luchinat, C.; Pierattelli, R. *J. Biomol. NMR* **2005**, *33*, 137.
(58) Bertini, I.; Felli, I. C.; Gonnelli, L.; Pierattelli, R.; Spyranti, Z.; Spyroulias, G. A. *J. Biomol. NMR* **2006**, *36*, 111–122.
(59) Pasat, G.; Zintsmaster, J. S.; Peng, J. *J. Magn. Reson.* **2008**, *193*, 226–232.
(60) Bertini, I.; Jiménez, B.; Pierattelli, R.; Wedd, A. G.; Xiao, Z. *Proteins: Struct., Funct., Genet.* **2008**, *70*, 1196–1205.
(61) Morris, G. A.; Freeman, R. *J. Am. Chem. Soc.* **1979**, *101*, 760–762.
(62) Müller, L. *J. Am. Chem. Soc.* **1979**, *101*, 4481–4484.
(63) Bodenhausen, G.; Ruben, D. J. *Chem. Phys. Lett.* **1980**, *69*, 185–188.
(64) Serber, Z.; Richter, C.; Moskau, D.; Boehlen, J.-M.; Gerfin, T.; Marek, D.; Haeberli, M.; Baselgia, L.; Laukien, F.; Stern, A. S.; Hoch, J. C.; Dötsch, V. *J. Am. Chem. Soc.* **2000**, *122*, 3554–3555.
(65) Pervushin, K.; Eletsky, A. *J. Biomol. NMR* **2003**, *25*, 147–152.
(66) Shimba, N.; Kovacs, H.; Stern, A. S.; Nomura, A. M.; Shimada, I.; Hoch, J. C.; Craik, C. S.; Dötsch, V. *J. Biomol. NMR* **2005**, *30*, 175–179.
(67) Farès, C.; Amata, I.; Carlomagno, T. *J. Am. Chem. Soc.* **2007**, *129*, 15814–15823.
(68) Fiala, R.; Sklenar, V. *J. Biomol. NMR* **2007**, *39*, 152–163.
(69) Morshauser, R. C.; Zuiderweg, E. R. P. *J. Magn. Reson.* **1999**, *139*, 232–239.
(70) Cavanagh, J.; Fairbrother, W. J.; Palmer, A. G., III; Rance, M.; Skelton, N. J. *Protein NMR Spectroscopy. Principles and Practice*; Academic Press: San Diego, CA, 2007; Chapter 5, pp 323−326, 549−552.
(71) Jeannerat, D. *J. Magn. Reson.* **2007**, *186*, 112–122.
(72) Bertini, I.; Duma, L.; Felli, I. C.; Fey, M.; Luchinat, C.; Pierattelli, R.; Vasos, P. R. *Angew. Chem., Int. Ed.* **2004**, *43*, 2257–2259.
(73) Emsley, L.; Bodenhausen, G. *Chem. Phys. Lett.* **1990**, *165*, 469–476.
(74) Boehlen, J.-M.; Bodenhausen, G. *J. Magn. Reson., Ser. A* **1993**, *102*, 293–301.

11.3 kHz strength). The ^{1}H and ^{15}N carriers are placed at 4.7 and 125 ppm, respectively. The ^{13}C band selective pulses on C^{ali}, C^{α}, and C' were given at the center of each region, respectively, and the adiabatic pulse was adjusted to cover all of the ^{13}C region. Decoupling of ^{1}H and ^{15}N was achieved with waltz-16[75] (1.7 kHz) and garp-4[76] (1.0 kHz) sequences, respectively. All experiments employ the IPAP approach to suppress the $C^{\alpha}-C'$ coupling in the direct acquisition dimension[56,77,78] where the in-phase (IP) and antiphase (AP) components are acquired and stored separately, doubling the number of FIDs recorded in one of the indirect dimensions.[38] The phase cycle, the method used for quadrature detection, the duration of the delays shown in the pulse sequences, and the relative strengths of the gradients used (all gradients had a duration of 1 ms and a sine shape) are reported case-by-case.

The CT HC HSQC experiment was chosen to determine the "nonselective" and the "selective" inversion recovery profiles of alpha (H^{α}) or aliphatic (H^{ali}) protons. In the "selective" experiment, the initial inversion element included a Q3-shaped band-selective 180° ^{13}C pulse of 860 μs (at 55 or 43 ppm) or of 220 μs (at 39 ppm) and a delay Δ_1 of about $1/J_{CH} \cong 6.8$ ms. The HN HSQC was chosen to determine the "selective" inversion recovery profiles of amide (H^{N}) protons (using in the initial inversion element a rectangular 180° ^{15}N pulse of 76 μs, at 118 ppm and a delay Δ_1 of about $1/J_{NH} \cong 11$ ms) and their "nonselective" analogues. The experiments were acquired with standard parameters, using an inter scan delay of 5 s to ensure complete recovery to thermal equilibrium. For each series (H^{α} "selective", H^{ali} "selective", the "nonselective" analogue, H^{N} "selective", and the "nonselective" analogue), eight experiments were recorded with the inversion recovery delay (τ) of 0.0001, 0.1, 0.2, 0.35, 0.5, 0.8, 1.2, and 2 s.

A variety of ^{13}C direct detection multidimensional NMR experiments were modified by including the "^{1}H-start" and subsequently the "^{1}H-flip", described in detail in the following section, to increase the sensitivity of the experiment and to reduce the inter scan delay, both effects contributing to the reduction of the amount of time needed to detect specific types of internuclear correlation NMR experiments.

For each type of 2D experiment ($C^{\alpha}-C'$ or $C'-N$ selected in our case), several series were acquired to evaluate the effect of the inclusion of the "^{1}H-start" and "^{1}H-flip", and, for each type of pulse sequence, the experiment was repeated several times by reducing the inter scan delay (3, 2.5, 1.5, 1.2, 0.9, 0.7, 0.5, 0.35, 0.23 s). In particular, the $C^{\alpha}-C'$ correlation map was acquired with the standard "^{13}C-start" version (CACO), with the "^{1}H-start" version ((H)CACO), and with the "^{1}H-flip" version ((H-flip)CACO). The common acquisition parameters were two scans per increment, spectral widths of 50 (aq) × 40 (^{13}C) ppm with 1024 × 256 data points in the direct and indirect acquisition dimensions.

The $C'-N$ correlation experiment was acquired with the standard "^{13}C-start" version (CON), with the version that exploits the "^{1}H-start" as a starting polarization source ((H)CON) as well as with the implementation of the "^{1}H-flip" ((H-flip)CON). The common parameters were eight scans per increment, spectral widths of 50 (aq) × 50 (^{15}N) ppm with 1024 (aq) × 512 (^{15}N) data points in the direct and indirect acquisition dimensions. For the ((H-flip)CON) experiment, the S/N allowed one to reduce the number of scans to two per increment.

Some of the 2D NMR experiments with the short inter scan delay were also acquired with a smaller spectral width in the indirect dimension, reducing the acquired data points by the appropriate factor, to maintain the resolution while reducing the experimental time necessary (20 and 10 ppm for the $^{13}C^{\alpha}$ indirect dimension and 20, 15, 12.5 ppm for the indirect ^{15}N dimension).

As an example of the reduction in experimental NMR time that can be obtained thanks to the implementation of the above-mentioned approaches, the 3D CANCO was acquired with the "^{1}H-start" version ((H)CANCO) as well as with the "^{1}H-flip" version ((H-flip)CANCO) by also making use of folding in the indirect acquisition dimensions. The (H)CANCO version was acquired with 16 scans per increment, an inter scan delay of 1.4 s, spectral widths of 50 (aq) × 35 (^{15}N) × 50 (^{13}C) ppm with 1024 (aq) × 64 (^{15}N) × 160 (^{13}C) data points. The (H-flip)CANCO version was acquired with 16 scans per increment, an inter scan delay of 330 ms, spectral widths of 50 (aq) × 15 (^{15}N) × 27 (^{13}C) ppm with 1024 (aq) × 64 (^{15}N) × 160 (^{13}C) data points. For the MDD version of the (H-flip)CANCO, the NUSSAMPLER program was used to generate the sampling table for acquisition. Spectra were recorded with either 20% or 40% of the complete set of increments. The resulting experimental data recorded according to the generated values were processed using MDD software included in the Bruker TopSpin 3.0 software. All other data were acquired and processed using the Bruker TopSpin 1.3 software.

The 3D CBCACON was also implemented in the "^{1}H-flip" version ((H-flip)CBCACON) and was compared to the available "^{1}H-start" version ((H)CBCACON). The two experiments were acquired with eight scans per increment, with an inter scan delay of 400 ms, spectral widths of 50 (aq) × 35 (^{15}N) × 80 (^{13}C) ppm with 1024 (aq) × 128 (^{15}N) × 200 (^{13}C) data points.

Results and Discussion

Implementation of the Pulse Sequences. It is well-known that the selective manipulation of a subset of proton spins in a protein yields significantly shortened longitudinal relaxation times.[70,79] The difference between the so-called selective and nonselective longitudinal relaxation profiles gives a measure of the expected gain in implementing relaxation enhanced sequences.[23,25−27,80]

The determination of selective and nonselective inversion recovery profiles for different kinds of ^{1}H spins in an isotopically labeled (^{13}C and ^{15}N) protein can be obtained using the basic strategy[81−84] schematically illustrated in Figure 1. Let us consider the general case of a proton spin H that has a large scalar coupling J_{HX} to a heteronuclear spin X, and of a second proton spin K that does not have a large scalar coupling with X (Figure 1A). The spin H can be selectively inverted with respect to spin K by using the building block shown in Figure 1B. Both spins H and K can be inverted by a simple spin echo (Figure 1C). This method can thus be used to determine selective (B) and nonselective (C) inversion recovery profiles for a spin H with respect to a spin K by repeating the experiments several times increasing the delay τ. The two building blocks can be used in a 1D spectrum by adding a 90° ^{1}H pulse at the end of the block. Alternatively, the two building blocks can be inserted prior to the beginning of a 2D pulse sequence when it is necessary to achieve a sufficient resolution for protein applications.

The same simple concepts can be used to control the spin-state of different types of ^{1}H spins (such as, for example, alpha,

(75) Shaka, A. J.; Keeler, J.; Freeman, R. *J. Magn. Reson.* **1983**, *53*, 313–340.
(76) Shaka, A. J.; Barker, P. B.; Freeman, R. *J. Magn. Reson.* **1985**, *64*, 547–552.
(77) Andersson, P.; Weigelt, J.; Otting, G. *J. Biomol. NMR* **1998**, *12*, 435–441.
(78) Ottiger, M.; Delaglio, F.; Bax, A. *J. Magn. Reson.* **1998**, *131*, 373–378.
(79) Neuhaus, D.; Williamson, M. *The Nuclear Overhauser Effect in Structural and Conformational Analysis*; VCH: New York, 1989; pp 123−140.
(80) Schanda, P.; Kupce, E.; Brutscher, B. *J. Biomol. NMR* **2005**, *33*, 199–211.
(81) Burum, D. P.; Ernst, R. R. *J. Magn. Reson.* **1980**, *39*, 163–168.
(82) Bendall, M. R.; Pegg, D. T.; Doddrell, D. M.; Field, J. *J. Am. Chem. Soc.* **1981**, *103*, 934–936.
(83) Freeman, R.; Mareci, T. H.; Morris, G. A. *J. Magn. Reson.* **1981**, *42*, 341–345.
(84) Garbow, J. R.; Weitekamp, D. P.; Pines, A. *Chem. Phys. Lett.* **1982**, *93*, 504–509.

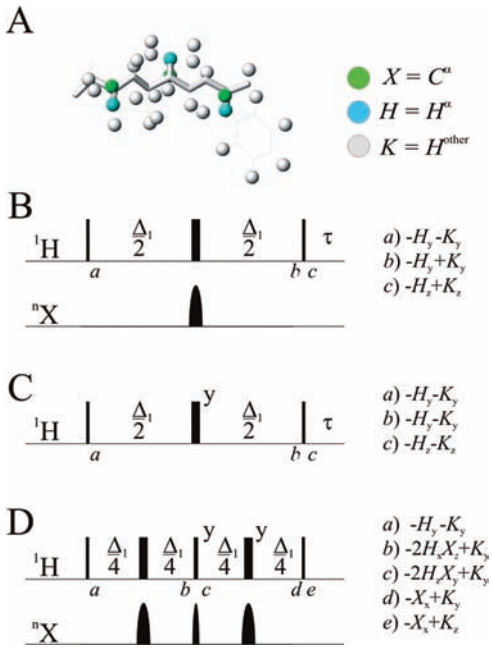

Figure 1. (A) Schematic representation of the backbone of a protein highlighting the C^{α} and H^{α} nuclei as well as other neighboring proton nuclei in the surroundings (residues 4−6 of ubiquitin, PDB code 1DZ3, are shown). The pulse sequence element (B) to achieve selective inversion of a set of proton spins H that have a large scalar coupling J_{HX} to a heteronuclear spin X and (C) to invert both kinds of spins H and K, where K represent proton spins that do not have a large scalar coupling with X (the delay Δ_1 is matched to $1/J_{HX}$ and, when not indicated explicitly, pulses have phase x). This can be used to determine selective and nonselective inversion recovery profiles of proton spins H. (D) The pulse sequence element that can be incorporated into exclusively heteronuclear experiments on the basis of ^{13}C detection to enhance the initial polarization of the heteronucleus X through a $H-X$ refocused INEPT transfer step (^1H-start) and to flip back along the z axis (^1H-flip) the magnetization of all other proton spins that do not have a large on-bond coupling with X (spins K in our example).

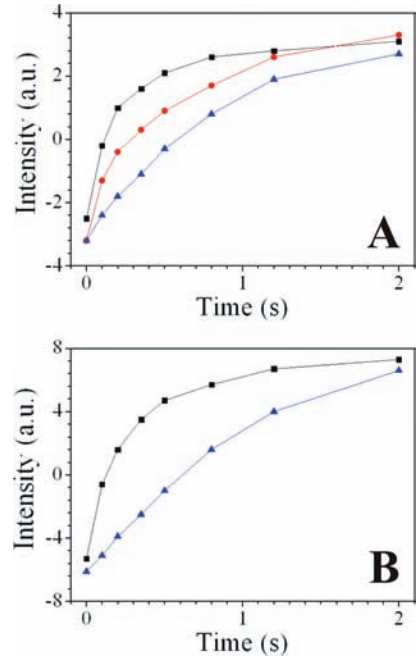

Figure 2. (A) Inversion recovery profiles of the H^{α} of residue 50 acquired with different initial conditions: selective H^{α} inversion (■), selective aliphatic inversion (●), and after inversion of all spins (▲); (B) recovery of one H^N signal either selectively inverting amide protons (■) or inverting all protons simultaneously (▲). Other profiles are reported in the Supporting Information (Figure S1).

aliphatic, aromatic, amide protons) in exclusively heteronuclear NMR ^{13}C direct detection experiments that exploit protons as a starting polarization source to increase the sensitivity of the experiments through an INEPT transfer step (^1H-start).[54] Indeed, in this kind of experiment, protons are perturbed at the beginning of the pulse sequence and when it is necessary to refocus $X-H$ scalar couplings during evolution or coherence transfer periods. In these conditions, in the initial part of the experiments, the proton spins that are not directly involved in the INEPT transfer can be flipped back to the $+z$ axis by including a ^1H 90° pulse at the end of the refocused INEPT transfer step. This approach permits one to enhance the longitudinal recovery of the proton spins providing the initial polarization transfer and thus to reduce the interscan delay. This is schematically shown in Figure 1D. In the subsequent parts of more complex pulse sequences, if a 180° inversion pulse is needed to refocus the evolution of $H-X$ scalar couplings, this can always be compensated by a 180° pulse of opposite phase close by in the pulse sequence to flip back the ^1H magnetization along the $+z$ axis (^1H-flip).

This experimental approach that exploits the evolution of one large heteronuclear scalar coupling to selectively invert one type of proton spins with respect to the others is an alternative as compared to the use of ^1H band-selective pulses proposed for ^1H direct detection multidimensional NMR experiments.[25,27,31] It is particularly well suited for exclusively heteronuclear NMR experiments based on ^{13}C detection because, as mentioned in the previous paragraph, protons are only used as a starting polarization source. However, it may be of general interest also for ^1H detected NMR experiments. It may be particularly advantageous when the selected proton types to be inverted are not easily manipulated through band-selective pulses due to signals overlap. This is the case, for example, for H^{α} spins, which resonate in a region very close to that of other aliphatic protons. The problem of overlap between the two chemical shift regions is reduced when analyzing the directly bound carbon spins, because the latter are characterized by a larger chemical shift dispersion.

Longitudinal Relaxation Enhancement. Following the approach outlined above, ^1H inversion recovery profiles were measured for H^{α} and amide protons of ubiquitin inserting the building blocks reported in Figure 1 at the beginning of the 2D HSQC pulse sequences ($^1H-^{13}C$ and $^1H-^{15}N$, respectively). For the acquisition of H^{α} inversion recovery profiles, the delay Δ_1 was set to $1/J_{CH} \cong 6.8$ ms, and the selectivity of the ^{13}C inversion pulse (either band-selective on the C^{α} region or on all of the aliphatic region) was exploited to invert only H^{α} protons or all aliphatic protons. Nonselective inversion recovery profiles were also acquired. The inversion recovery profiles determined for H^{α} protons under different initial conditions (inversion of H^{α} only, of all aliphatic protons, or of all protons) can thus be compared. As an example, the recovery of the H^{α} of residue 50 is reported in Figure 2A. It can be observed that the time point for which the intensity of an NMR signal crosses zero in an inversion recovery experiment (T_{null}) decreases from about 500 ms to 250 ms to 100 ms, by progressively restricting the ensemble of inverted spins, indicating a faster recovery to equilibrium of the observed spins. For amide protons, the delay Δ_1 should be set to $1/J_{NH} \cong 11$ ms, and a square 180° is used to invert amide ^{15}N spins. Two inversion recovery profiles were determined inverting either only amide protons or all protons simultaneously. As an example, the data for residue 50 are

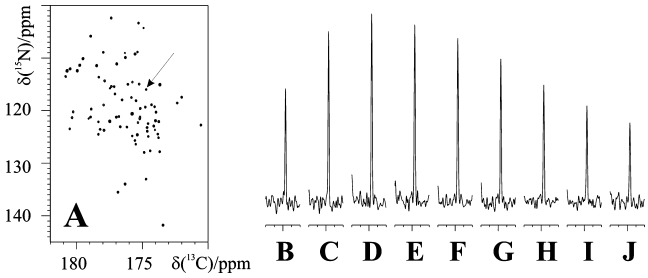

Figure 3. The intensity of one of the cross peaks obtained in 2D CON experiments (the correlation for C′59−N60 of ubiquitin indicated by an arrow in the full spectrum reported in (A)) recorded with different pulse schemes and different interscan delays (d_1) is compared by showing its trace. From left to right: (B) ^{13}C start ($d_1 = 2.5$ s), (C) ^{1}H start ($d_1 = 1.5$ s), and (D)−(J) H^{α}-flip with different relaxation delays d_1 (1.5, 1.2, 0.9, 0.7, 0.5, 0.35, 0.2 s).

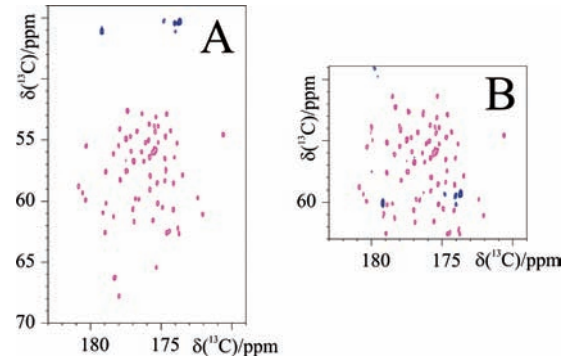

Figure 4. Parts of the 2D CACO maps recorded on ubiquitin with the (H-flip)CACO experiment in (A) 3 min and (B) 1 min. All of the correlations detected in (A) are also observed in (B); a few additional correlations from side-chains (Asx, Glx) are present in (B) due to spectral folding in the indirect dimension, while in (A) they are outside the printed area.

shown in Figure 2B. Also in this case, the T_{null} decreases from about 500 to about 100 ms, indicating a pronounced effect of the same magnitude as that observed for H^{α} spins.

A similar behavior is observed for the majority of residues in well-structured regions of the protein (Figures S1 and S2 of the Supporting Information). The differential longitudinal relaxation effect, which depends on the local correlation time, is less pronounced for the first and last residues, as well as for some residues in external loops (Figures S1 and S2 of the Supporting Information), which are characterized by higher local mobility and, for this reason, are anyway characterized by a faster recovery to equilibrium.

The determined inversion recovery profiles show that the proposed approach works and that it can be exploited to significantly enhance the longitudinal recovery of ^{1}H polarization in exclusively heteronuclear NMR experiments based on ^{13}C direct detection, through the implementation of the building block shown in Figure 1D. Several examples will be given in the next sections starting from the most sensitive and useful 2D experiments (CON and CACO) and then moving to some of the most useful 3D experiments.

CON and CACO Experiments. The 2D H^{α}-start CON experiment can be taken as an example to illustrate the approach. The insertion of the $H^{\alpha}-C^{\alpha}-CO$ transfer (^{1}H-start), which is a necessary additional block with respect to the basic pulse sequence,[37] allows one to significantly increase the sensitivity of the experiments. The modified pulse sequence to implement longitudinal relaxation enhancement (^{1}H-flip) is shown in the Supporting Information. This was used to acquire a series of spectra on ubiquitin, all recorded with the same number of scans, but with decreasing relaxation delay. These were then compared to the standard (H)CON experiment and with the ^{13}C-start experiment where the interscan was scaled to account for the increase in longitudinal recovery of ^{13}C as compared to ^{1}H (nonselective) by a factor of about 1.7, which was experimentally verified. As an example, the traces extracted from these 2D spectra for the C′59−N60 correlation are shown in Figure 3. It is worth noting that the proposed variant of the CON provides the same S/N as the standard experiment about 1/5 of the time and that all of the expected resonances can be detected, proving the generality of the approach.

The large chemical shift dispersion typical of heteronuclei provides well-dispersed spectra. The possibility given by this experiment to observe signals involving proline residues further increases the chemical shift dispersion of the correlations, particularly in the ^{15}N dimension, minimizing the occurrence of overlap (Figure 3A). As a result, even if ^{15}N signals resonate in a large chemical shift range (from about 105 ppm for glycines residues to about 145 ppm for proline residues), it is possible to use extensive spectral aliasing to reduce the actual spectral width and thus the number of points acquired in the indirect dimension without losing resolution. The spectral width in the ^{15}N dimension could be reduced by a factor of about 3, without increasing the number of peaks in overlap (not shown). The consequent reduction in terms of experimental time, still keeping the same resolution in the indirectly detected dimension, is thus a factor of about 3. Indeed, the number of acquired data points necessary to maintain the same resolution in the indirect dimension is reduced by the same factor by which the spectral width is reduced.

In summary, the combination of longitudinal relaxation enhancement and spectral aliasing, which constitute two independent approaches to reduce experimental time, contributes to a reduction of experimental time, which permits one to acquire a CON experiment in about 5 min.

Similarly, the $^{1}H^{N}$-start, $^{1}H^{N}$-flip versions of the CON experiment ((NH-flip)CON) can be implemented. However, the (H-flip)CON experiment, which uses H^{α} polarization as a starting source, is less prone to losses due to exchange processes as compared to a (NH-flip)CON, and it allows one to detect proline residues. Therefore, it is generally preferred to the versions that start with $^{1}H^{N}$ polarization, even if the latter is in principle more sensitive. The same argument holds when comparing the performance of the proposed experiments to the ^{1}H detected experiments that provide similar information (3D HNCO).

Another example can be provided by the most simple and sensitive exclusively heteronuclear NMR experiment based on carbonyl direct detection, the CACO. This experiment gives information on C′ and C^{α} of all amino acid types and thus provides highly complementary information to that obtained though a CON experiment. Therefore, it may be a useful complement to $^{1}H-^{15}N$ HSQC experiments to complete the study of the properties of backbone nuclei that cannot be obtained though simple 2D experiments based on ^{1}H direct detection. For example, it may be profitably used for chemical shift mapping and alike applications.[58]

The inclusion of proton polarization as a starting source as well as the implementation of the longitudinal relaxation rate enhancement are analogous to that discussed in the previous

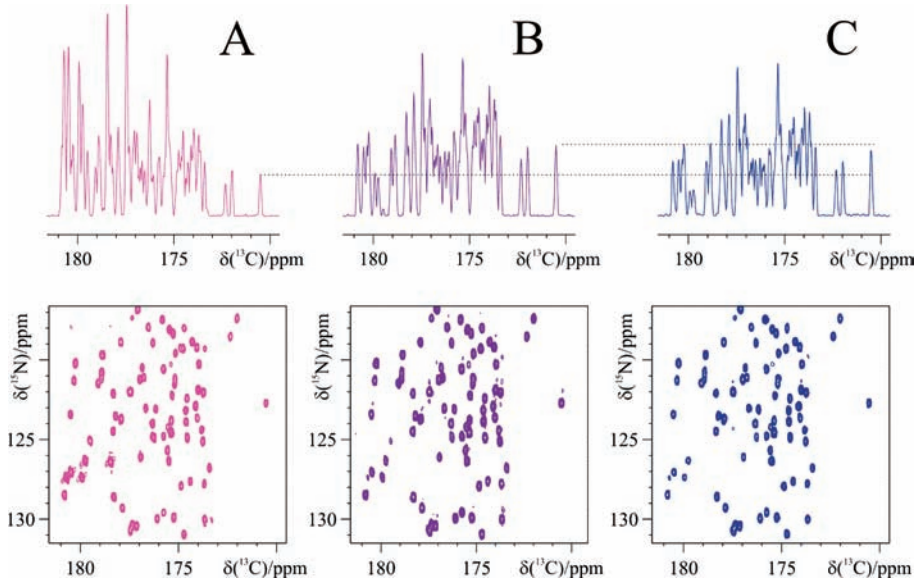

Figure 5. C′−N projections of the 3D CANCO maps acquired with the (H)CANCO (A) and the (H-flip)CANCO (B) pulse sequences in the same experimental time. The 1D projections reported in the upper part clearly show the increase in intensity obtained with the "^{1}H-flip" version. In (C), the C′−N projection of the MDD (H-flip)CANCO map recorded with the same experimental parameters as the map reported in (B) but sampling only 40% of the increments in the indirect dimensions is shown. The reduction in the overall intensity of the 1D projection is almost negligible.

paragraph (the relevant pulse sequences are reported in the Supporting Information). A (H-flip)CACO spectrum as the one reported in Figure 4A showing all of the expected correlations for ubiquitin can be recorded in about 3 min. With the exploitation of spectral folding in the indirect dimension (Figure 4B), the time necessary for acquisition is further reduced to 1 min.

Implementation in 3D Experiments. Spectral folding and longitudinal relaxation rate enhancement can be incorporated in virtually any ^{1}H-start, ^{13}C detect, exclusively heteronuclear NMR experiment through the inclusion of the building block described in Figure 1D. As an example, the modified pulse sequence for the (H-flip)CANCO is shown in the Supporting Information. An experiment with a good resolution and high S/N could be acquired in 11 h. Careful inspection of the 3D maps shows that all expected correlations could be detected through this variant of the CANCO. As an example of the quality of the data, the C′−N projections of the standard (H)CANCO spectrum and of the new variant of (H-flip)CANCO recorded in the same amount of time (see Experimental Data) are shown in Figure 5A and B, respectively. The 1D projections on the upper part of the figure compare the relative intensity of the ensemble of the cross peaks, and they clearly demonstrate the gain in sensitivity obtained in the unit time employing longitudinal relaxation enhancement and spectral folding in the indirect dimensions. The same "^{1}H-flip" approach can obviously be also included in the "selective" CANCO,[85] the complementary experiment to clearly identify and discriminate between intra- and inter-residue correlations.

Similarly, the (H)CBCACON experiments,[54] used for the identification of ^{13}C resonances of each amino acid and for correlating them with the nitrogen of the following residue, can be converted to the "^{1}H-flip" variant, even if the gain deriving from the implementation of longitudinal relaxation enhancement is expected to be smaller as all aliphatic nuclei provide the initial polarization source (instead of only H^α nuclei, as in the previous examples). Despite this, thanks to the combination of "^{1}H-start" and "^{1}H-flip", a 3D spectrum could be acquired in 6 h.

These 3D experiments are perfectly suited to be combined with so-called fast acquisition techniques.[4,6−11,20,86−89] These methods rely on the assumption that, with a proper choice of the experimental parameters, it is possible to reconstruct a full multidimensional data set from a reduced set. We tested the method of nonuniform sampling using MDD for processing.[6,9,16,20] Conventionally, all of the points in the indirect dimensions that fall on the grid given by the Nyquist theorem are sampled. In nonuniform sampling, only a subset of those is recorded in a random fashion. These points can either be distributed equally or exponentially weighted, such as to sample more at the beginning of the FID, when the S/N is high. Nonuniform sampling allows one to reduce the number of data points acquired in the indirect dimensions, optimizing the resolution and the sensitivity for a given experimental time. The data are then processed using MDD algorithms[6,9,16,20] instead of the standard fast Fourier transform algorithm. Alternatively, maximum entropy algorithms[13,18] or Fourier transform algorithms for nonequidistant data[13,15] can be used.

Taking again the CANCO experiments as an example, because it is one of the most demanding experiments in term of sensitivity, we proved that a reduction in sampled data points to build the 3D map to about 40% allows one to obtain a 3D experiment displaying all of the expected correlations necessary for sequence-specific assignment. The C′−N projection of the obtained 3D map is reported in Figure 5C for comparison. At the current stage of technology, it is not possible to go below this 40% threshold, as the reduced S/N of the MDD spectrum

(85) Bermel, W.; Bertini, I.; Felli, I. C.; Pierattelli, R.; Vasos, P. R. *J. Magn. Reson.* **2005**, *172*, 324–328.
(86) Szyperski, T.; Wider, G.; Bushweller, J. H.; Wüthrich, K. *J. Am. Chem. Soc.* **1993**, *115*, 9307–9308.
(87) Freeman, R.; Kupce, E. *J. Biomol. NMR* **2003**, *27*, 101–113.
(88) Atreya, H. S.; Szyperski, T. *Methods Enzymol.* **2005**, *394*, 78–108.
(89) Kupce, E.; Freeman, R. *J. Magn. Reson.* **2008**, *191*, 164–168.

causes the appearance of artifacts that may cause misassignments. However, this is the proof that ^{13}C direct detection experiments are as versatile as are the inverse-detected experiments.

Conclusions

Carbon-13 direct detection NMR is becoming a widely usable spectroscopy that can fruitfully complement ^{1}H NMR spectroscopy in the investigation of biomolecules. With the increase in sensitivity nowadays obtained with modern spectrometers, ^{13}C direct detection NMR can further benefit by the implementation of the so-called fast methods to reduce the experimental time. We have shown that with a standard 0.5 mM sample of a protein, it is possible to record the basic 2D experiments in a few minutes, while 3D experiments can be recorded in a few hours, a result unconceivable until a few years ago. As the technology progresses, it can be expected that experiments will become less and less demanding in terms of experimental effort.

Acknowledgment. This work has been supported in part by the EC contracts EU-NMR no. 026145 and SPINE II no. 031220, FIRB-Proteomica RBRN07BMCT and by Ente Cassa di Risparmio di Firenze. Dr. Vladislav Yu. Orekhov and Dr. Victor A. Jaravine are gratefully acknowledged for providing the software for NUS and MDD acquisition and data analysis. Dr. Bernhard Brutscher is acknowledged for stimulating discussions.

Supporting Information Available: (H-flip)CON, (H-flip)-CACO, and (H-flip)CANCO pulse sequences, details of experimental parameters used, and two figures to illustrate the differential proton relaxation properties in ubiquitin. This material is available free of charge via the Internet at http://pubs.acs.org.

JA9058525